INTERNATIONAL ATOMIC ENERGY AGENCY
UNITED NATIONS EDUCATIONAL, SCIENTIFIC AND CULTURAL ORGANIZATION
INTERNATIONAL CENTRE FOR THEORETICAL PHYSICS
I.C.T.P., P.O. BOX 586, 34100 TRIESTE, ITALY, CABLE: CENTRATOM TRIESTE

UNITED NATIONS INDUSTRIAL DEVELOPMENT ORGANIZATION

INTERNATIONAL CENTRE FOR SCIENCE AND HIGH TECHNOLOGY
c/o INTERNATIONAL CENTRE FOR THEORETICAL PHYSICS 34100 TRIESTE (ITALY) VIA GRIGNANO, 9 (ADRIATICO PALACE) P.O. BOX 586 TELEPHONE 040-224572 TELEFAX 040-224575 TELEX 460449 APH I

SMR/760-5

"College on Atmospheric Boundary Layer and Air Pollution Modelling"
16 May - 3 June 1994

"Hybrid Plume Dispersion Model (HPDM) Development and Evaluation"

S. HANNA
Environmental Research and Technology, Inc.
Concord, Massachusetts
USA

Please note: These notes are intended for internal distribution only.

2.1

Hybrid Plume Dispersion Model (HPDM) Development and Evaluation

STEVEN R. HANNA

Sigma Research Corporation, Westford, Massachusetts

ROBERT J. PAINE

ERT, Concord, Massachusetts

(Manuscript received 4 June 1988, in final form 26 September 1988)

ABSTRACT

The Hybrid Plume Dispersion Model (HPDM) was developed for application to tall stack plumes dispersing over nearly flat terrain. Emphasis is on convective and high-wind conditions. The meteorological component is based on observational and modeling studies of the planetary boundary layer. The dispersion estimates for the convective boundary layer (CBL) were developed from laboratory experiments and field studies and incorporate convective scaling, i.e., the convective velocity scale, w_*, and the CBL height, h, which are the relevant velocity and length scales of the turbulence. The model has a separate component to handle the dispersion of highly buoyant plumes that remain near the top of the CBL and resist downward mixing. For convective conditions, the vertical concentration distribution is non-Gaussian, but for neutral and stable conditions it is assumed to be Gaussian. The HPDM performance is assessed with extensive ground-level concentration measurements around the Kincaid, Illinois, and Bull Run, Tennessee, power plants. It was also tested with limited data during high-wind conditions at five other power plants. The model is found to be an improvement over the standard regulatory model, MPTER, during light-wind convective conditions and high-wind neutral conditions.

1. Introduction

In a review of models for calculating atmospheric dispersion, Smith (1984) reported that models used for regulatory applications are generally many years behind the state of the art and produce predictions that do not agree well with observations. Similar findings were reported by Hayes and Moore (1986), who summarized 15 model evaluation studies. Several regulatory models were tested by Bowne et al. (1983, 1985) with the Kincaid, Illinois, and Bull Run, Tennessee, tracer datasets used in our model development project. For example, an equivalent of the Environmental Protection Agency (EPA) CRSTER model and two others were tested by Bowne et al. (1983) for their performance in an "operational" or "regulatory" application, i.e., for their ability to predict ground-level concentrations (GLCs) for specific averaging times—1, 3, 24 h—without regard to the validity or accuracy of individual model components (plume rise, dispersion parameters, etc.). When predicted and observed concentrations at the Kincaid site were unpaired in space and time, the CRSTER-equivalent model predicted the maximum hourly averaged SO_2 GLC to within 30% but overpredicted the SF_6 GLC by 35% to 70%; the other models performed about the same or worse. When the concentrations were paired in space and time, none of the models predicted the concentration field with any accuracy, e.g., the correlation coefficients between observed and predicted concentrations were often negative. In their evaluation of individual model components at the Kincaid and Bull Run sites, Liu and Moore (1984) and Moore et al. (1985) found that many did not perform well. For example, lidar observations of vertical dispersion, σ_z, were generally smaller than model predictions.

A set of review papers in the November 1985 issue of the *Journal of Climate and Applied Meteorology (JCAM)* summarized recent research on turbulence and dispersion in the planetary boundary layer and discussed its use in the development of improved models for dispersion applications. The results of most immediate use concerned dispersion in the convective boundary layer (CBL), in which the important length and velocity scales of the turbulence are the CBL depth, h, and the convective velocity scale, w_*:

$$w_* = \left(\frac{g\overline{w\theta}_0 h}{\bar{\theta}_0}\right)^{1/3} \tag{1}$$

Here, g is the gravitational acceleration, w and θ_0 are turbulent fluctuations in vertical velocity and potential temperature, $\overline{w\theta}_0$ is the surface kinematic heat flux, and $\bar{\theta}_0$ is the mean potential temperature at the surface.

Corresponding author address: Steven R. Hanna, Sigma Research Corp., 234 Littleton Road, Suite 2E, Westford, MA 01886.

© 1989 American Meteorological Society

The overbars refer to time averages over about 1 h. Note that the convective velocity scale is not dependent on the wind speed, u.

The emphasis on the CBL was driven in part by applications—the maximum GLCs from tall stacks generally occur during convection. One of the key recommendations from the *JCAM* papers was that w_* and h should be used directly in expressions for the lateral (σ_y) and vertical (σ_z) dispersion parameters since successful demonstration of this approach already had been made. Another suggestion was that the p.d.f. dispersion model, which is based on the probability density function (p.d.f.) of vertical velocity fluctuations (w), should be extended to buoyant plumes. In the CBL, the vertical velocity p.d.f. is non-Gaussian and accounts for the non-Gaussian nature of the vertical dispersion. A third recommendation was that a special treatment was required for the slow downward dispersion of highly buoyant plumes that loft near the top of the CBL.

In addition to the above, recommendations were given for planetary boundary layer (PBL) wind and turbulence profiles as well as methods for estimating key boundary layer variables: e.g., the surface heat and momentum fluxes, h (van Ulden and Holtslag 1985; Weil 1985). Recommendations were also given for dispersion in the stable boundary layer (Hunt 1985) and on concentration fluctuations and uncertainty; however, they were considered more for research and future model development than for immediate use.

Prior to the *JCAM* articles, several efforts took place to develop improved dispersion models based on PBL understanding. One was by Venkatram (1980), who developed an "impingement" model for buoyant plumes. The GLC distribution was found from an assumed p.d.f. of the impingement distance, which is where plume segments caught in downdrafts first touch the surface. The mean impingement distance was found from Briggs' (1975) touchdown model for plume rise. The model included convective scaling and showed good performance in an evaluation with field observations around tall stacks.

Other efforts were those of Weil and Brower (1984) and Berkowicz et al. (1985) who improved the Gaussian plume model by including dispersion parameters and stability estimation methods based on convective scaling ideas. Weil and Brower adopted Briggs' empirical dispersion curves, which were intended for elevated releases and were consistent with the short-range limit of statistical theory. They related the curves to u/w_* using interpolation expressions for the turbulence components, σ_v, σ_w. They included Briggs' (1975, 1984) formulations of final rise in convective conditions and partial plume penetration of elevated stable layers. An evaluation of their model with SO_2 GLC measurements around Maryland power plants showed that it performed much better than the EPA CRSTER model. However, a later evaluation by Tikvart et al. (1987) showed that it overestimated the maximum SO_2 concentrations around the Clifty Creek power plant by a factor of about 2. The overpredictions occurred for highly buoyant plumes that did not penetrate the elevated inversion and presumably did not disperse as a passive tracer (Weil and Corio 1985). Instead, such plumes tended to remain near the top of the CBL and disperse downward slowly over long distances.

Berkowicz et al. (1985) developed expressions for σ_y and σ_z explicitly in terms of w_*, u_*, h, z_0, and x, using statistical theory for elevated sources and an adaptation of it for surface-layer sources. Here, u_* is the friction velocity, z_0 is the surface roughness length, and x is the downwind distance. Evaluation of their model with GLCs from a few selected periods at the Kincaid plant showed satisfactory performance.

Researchers at the EPA followed some of the recommendations in Hanna et al. (1977) and the 1985 *JCAM* papers to formulate their Gaussian model, TUPOS (Turner et al. 1986). For example, they calculated dispersion parameters directly using statistical theory and vertical profiles of turbulence based on PBL parameterizations; in addition, they computed plume rise and partial penetration of elevated inversions using modeled profiles of wind and temperature. Gryning et al. (1987) used a combination of eddy-diffusion theory, statistical theory, and empirical parameterizations along with simple expressions for wind and turbulence profiles in terms of relevant PBL scaling variables to derive simple expressions for dispersion and concentration fields. Their model, applicable only to nonbuoyant sources, showed good agreement with observed dispersion and concentrations.

Other models have been developed or evaluated using portions of the Kincaid data base. One is the Berkowicz et al. (1985) model mentioned earlier. A second example is Pierce's (1986) testing of Briggs' (1985) empirical model for dispersion of highly buoyant plumes in the CBL. Although there was considerable scatter between observed and predicted GLC's, the performance statistics for the Briggs' model were substantially better than those of the EPA MPTER model. A third is that of Petersen et al. (1987) who tested their eddy-diffusion (K) model with two days of the Kincaid data. Their K values were prescribed in terms of turbulence velocity variances which were calculated from a second order closure model. The model performed satisfactorily under neutral to stable conditions but underpredicted the maximum of GLC's by a factor of two during convection; the authors attributed this partially to the inadequacy of K theory for treating dispersion in convection.

The purpose of the project described in this paper was to develop a new dispersion model for buoyant plumes from tall stacks, including as many of the new theoretical concepts as possible. The new model, called the Hybrid Plume Dispersion Model (HPDM), was intended for application in the regulatory setting (i.e.,

TABLE 1. Site characteristics and data collected.

Parameter	Kincaid	Bull Run
Terrain	Flat farmland, some lakes	Rolling 100 m forested hills, some lakes
Megawatts	1320	950
Stack height and diameter	187 m, 9.0 m	243 m, 9.0 m
SO_2 data	30 stations, operated for about one year	Not used
SF_6 data	200 monitors deployed on arcs from 0.5 to 50 km; location depends on met.; three 3-week periods.	200 monitors deployed on arcs from 0.5 to 50 km; location depends on met.; two 5-week periods.
Meteorological data	100 m tower (including *uvw* turbulence) doppler acoustic sounder, slow-rise temperature sounders, 10 m supplemental towers	
Lidar	Three types of lidar doing plume scans	Two types of lidar doing plume scans.

applications to a year of hourly data, where only routine meteorological data are available). HPDM was developed and evaluated primarily using field data from the Kincaid, Illinois, and Bull Run, Tennessee, power plants. It was also evaluated with a high-wind dataset from five other power plants. The following sections describe HPDM and its meteorological assumptions.

2. Field data used for model development and evaluation

Scientists, engineers, and technicians from several companies converged on the Kincaid, Illinois, power plant in 1980 and 1981, and the Bull Run, Tennessee, power plant in 1982 in order to collect meteorological and aerometric data to be used in the development and evaluation of transport and dispersion models for emissions from tall stacks. The Kincaid plant is surrounded by flat farmland and the Bull Run plant by rolling wooded terrain, typically 100 m high hills. For most of the observations, the basic averaging time was 1 h; the primary tracer material measured was SF_6 gas, which was released from the plant stacks. Bowne et al. (1983, 1984) summarized these observations, which are believed to be the most comprehensive of their type. The total data file from these experiments includes five Hertz turbulence data, 5-min SO_2 data, and lidar data from hundreds of plume scans. Table 1 lists the site characteristics and types of data collected. The 200 SF_6 monitors were shifted day-to-day to coincide with the forecasted wind direction and the expected distance to the maximum ground level concentration. Figure 1 shows a map of monitor positions at Kincaid for neutral conditions and westerly winds. For a wind speed of 5–10 m s^{-1}, the angular extent of the monitors should be sufficient to capture the entire plume. Thirty SO_2 monitors were also operated at Kincaid, and their positions are shown in Fig. 2. At Bull Run, where winds were lighter (typically about 2 m s^{-1}), the angular extent of the monitors was increased (Fig. 3 shows the monitor positions at Bull Run).

It was recognized that the data used to develop the new model should not be used in the final evaluation of the model. Consequently, the data were divided (by day) into two parts—a developmental database and an evaluation database. The evaluation database was not touched until the final model runs were made that are reported in this paper. These data are not truly independent, since the field site is unchanged and pollutant concentrations on one day could be correlated with those on the next. However, the database division was the best approach that could be followed without conducting experiments at more sites.

Most of the meteorological and aerometric observations in the developmental database were analyzed to some extent. In the analysis, it was discovered that some observations contained much more uncertainty than others. For example, the turbulence and PBL height measurements from the Doppler Acoustic Sounder (DAS) were unreliable during nighttime and transition periods. In addition, the turbulence measurements from a three-dimensional propeller ane-

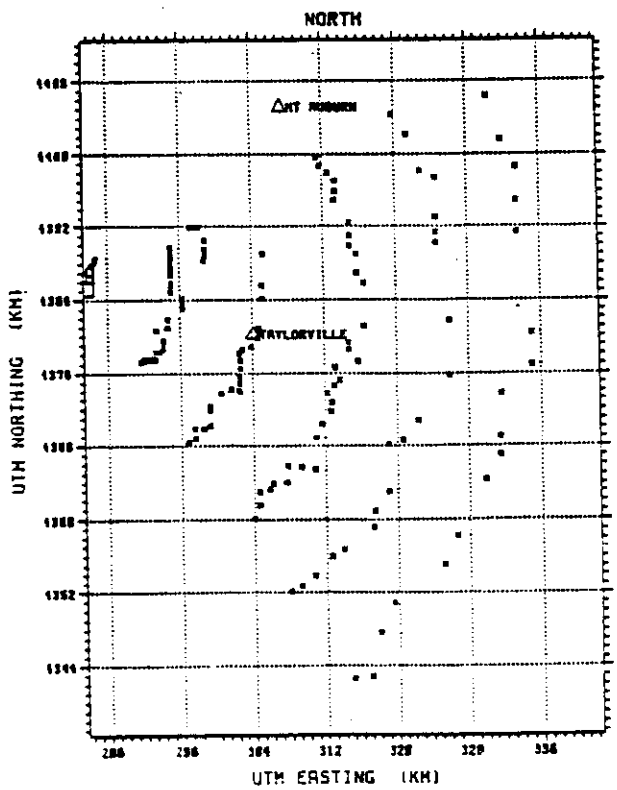

FIG. 1. The SF_6 tracer sampling array at Kincaid for neutral conditions and westerly winds.

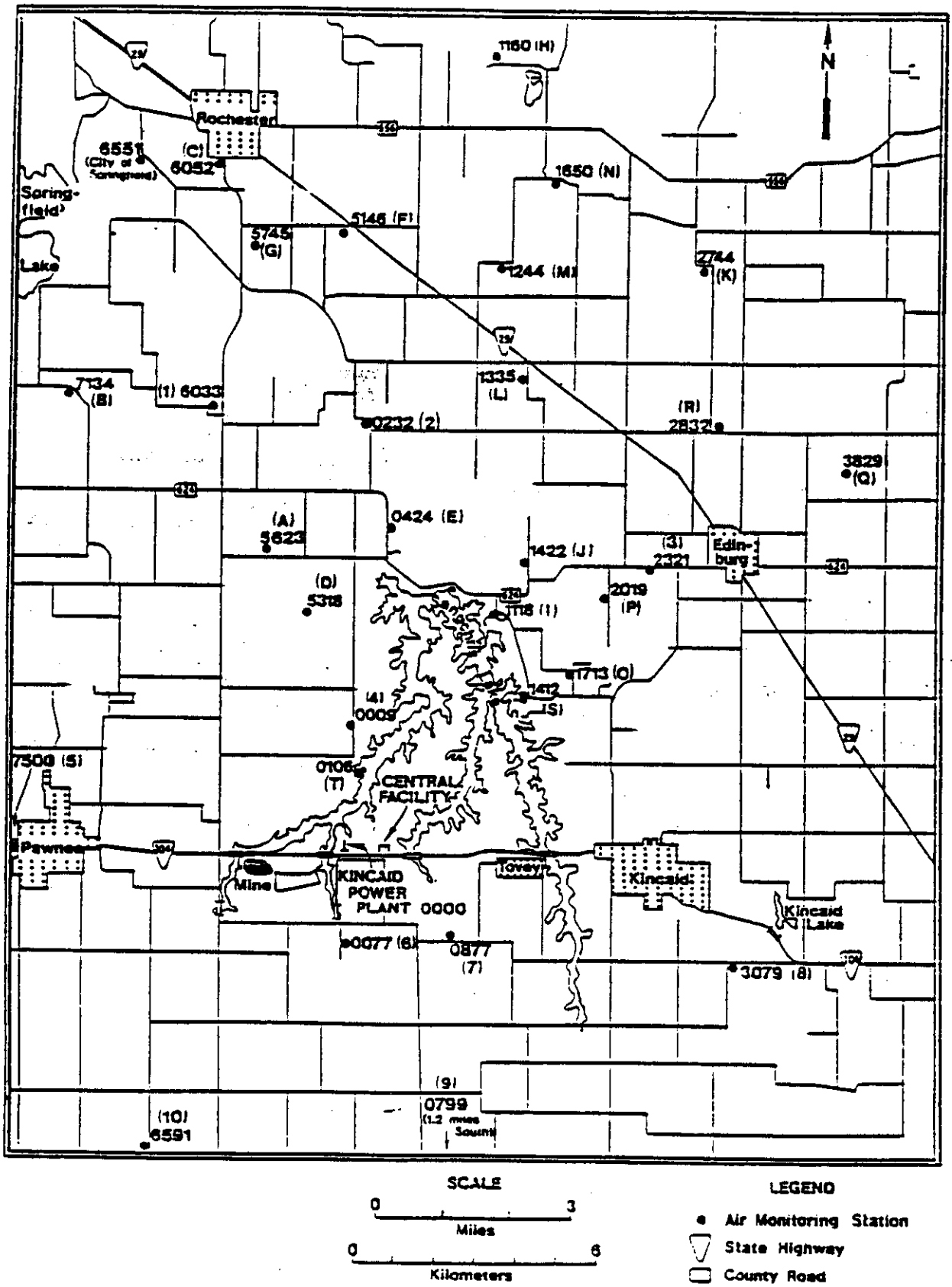

FIG. 2. The SO_2 receptor positions at Kincaid.

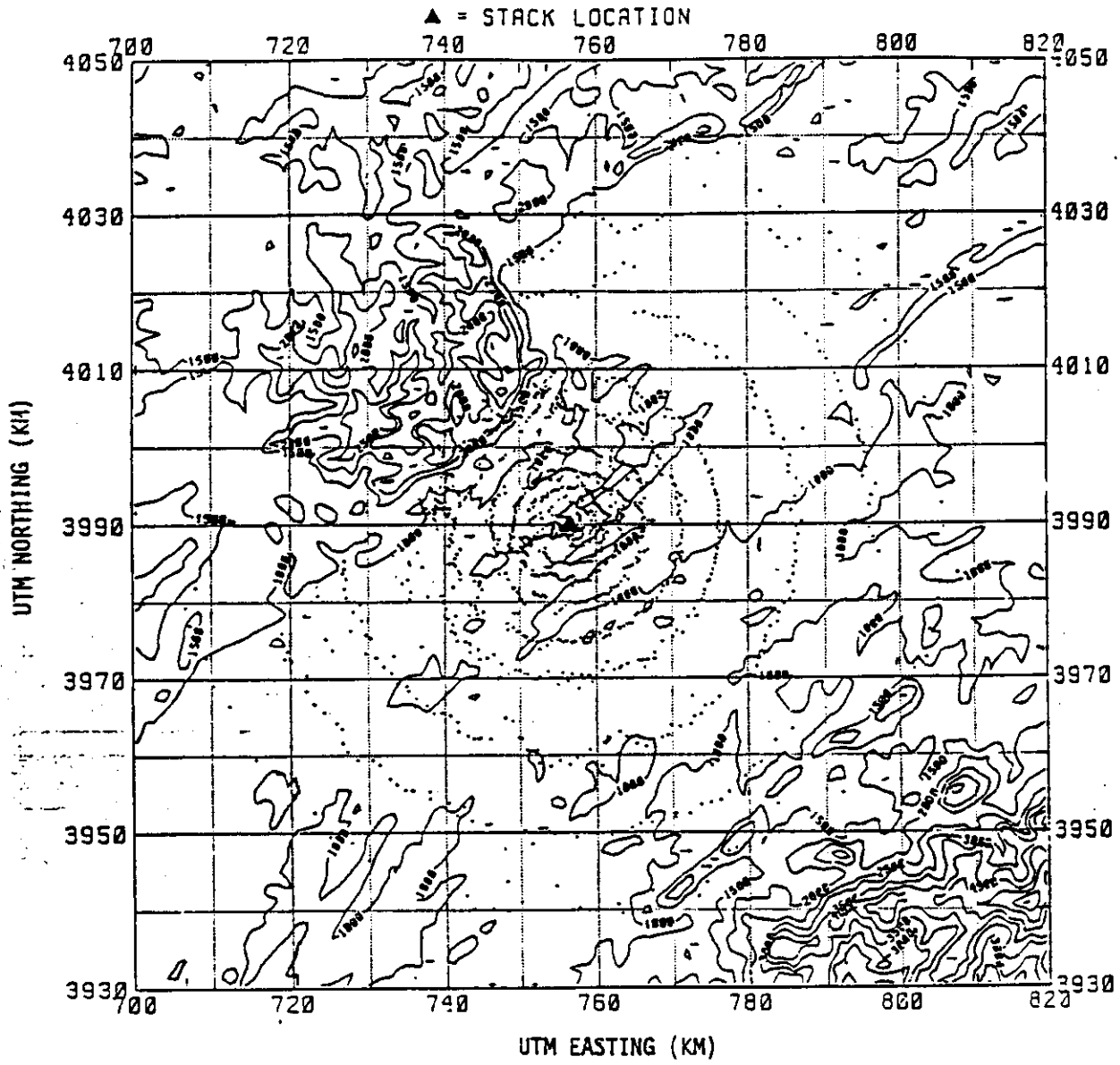

FIG. 3. Map of SF_6 tracer monitoring sites around the Bull Run steam plant.

mometer on the tower were found to have several unresolved problems including a mean vertical speed, $\bar{w}$, nearly equal to the standard deviation (σ_w). Other measurements such as the SF_6 concentrations and the wind speeds from cup anemometers on a tower were much more accurate. Table 2 presents a summary of the estimated uncertainties in some of the measurements. Note that a 6% error in the measured SF_6 concentration translates directly into a 6% discrepancy between observed and predicted concentrations.

3. The hybrid plume dispersion model (HPDM)

The maximum hourly averaged ground-level concentrations (GLCs) around tall stacks in flat terrain usually are observed during unstable conditions when plumes are dispersed by large-scale downdrafts and updrafts (section 1). The rate of dispersion depends not only on u, w_*, and h, but also on the plume buoyancy flux. Another meteorological situation that can lead to moderately high GLCs around tall stacks is high-wind, nearly-neutral conditions in which turbulence and dispersion are dominated by wind shear. This situation also can cause high GLCs over a 24-h period because it can persist for many hours with a quasi-steady wind direction. For tall stacks, the CRSTER model significantly underestimates concentrations during high-wind, nearly-neutral conditions because the modeled σ_z is too small (e.g., Venkatram and Paine 1985). In developing HPDM, we have focused on dis-

TABLE 2. Uncertainties in EPRI data, Kincaid site.

Parameter	Standard deviation of error	Method of determination
Monitored SF_6		
<100 ppt	6 ppt	Colocated samplers, duplicate analysis
≥100 ppt	6%	
Wind direction		
Vane on tower	2°	Alignment checks*
Various instruments	20°	Comparison between rawinsonde, DAS, and vane on tower
Wind speed (tower)	0.1 m s^{-1}	Turn cups by motor*
Turbulent speed (3-D props)	0.5 m s^{-1}	Comparison with cups
dT/dz (tower)	0.01°C/m	Tower versus sounding
Mixing height h		
Night DAS**	±100%	Comparison with sounding
Day temperature sounding	±10–20%	Analysis of sounding by three meteorologists

* The actual error is probably larger, since these numbers were determined by simple mechanical checks, rather than by intercomparisons between instruments.

** DAS = Doppler Acoustic Sounder.

persion in these two meteorological situations and on the estimation of the necessary PBL variables.

HPDM is intended to be applied in the same manner as EPA regulatory models such as CRSTER, MPTER, or ISC, and, therefore, must be computationally efficient. That is, it should calculate the hourly averaged GLCs at multiple downwind receptors over a 1-yr period and within a reasonable amount of computer time. In addition, it must be "user friendly" such that practitioners with a minimum of training can apply it. For these reasons HPDM was formulated in the basic framework of the MPTER model, which is familiar to the air quality modeling community. The equation for the ground-level concentration, C, has the general form:

$$C = \frac{QG_yG_z}{u} \tag{2}$$

where Q is the source emission rate, u is the mean wind speed, and G_y and G_z are concentration distribution functions in the lateral and vertical directions, respectively. Here G_z is evaluated at the surface, $z = 0$. As is customary with "steady" plume models, the source and meteorological conditions are assumed to be constant over the averaging time (1 h) and the travel time from the source to the receptor.

The lateral concentration distribution is assumed to be Gaussian for all stability conditions; i.e., G_y is given by

$$G_y = (\sqrt{2\pi}\,\sigma_y)^{-1} \exp(-0.5((y - y_p)/\sigma_y)^2) \tag{3}$$

where y_p is the lateral position of the plume centerline. The vertical distribution is assumed to be Gaussian only for stable and neutral conditions, which are defined in Section 3*a*; for these conditions, G_z is given by

$$G_z = (\sqrt{\pi/2}\,\sigma_z)^{-1} \exp(-0.5(z_p/\sigma_z)^2) \tag{4}$$

where z_p is the height of the plume centerline above the ground. Equation (4) accounts for plume reflection at the surface; image sources are added to account for plume reflection at the top of the boundary layer, $z = h$.

The dispersion parameters and plume height depend on the vertical profiles of wind, temperature, and turbulence in the PBL. In the following, we discuss methods for determining these profiles and then describe models for estimating the dispersion and plume height.

a. Boundary layer parameterization

Wind, temperature, and turbulence profiles can be provided to HPDM by detailed on-site observations if available. These data should be obtained within a kilometer or so of the source. However, since these observations generally are not available, we have included formulas for modeled or parameterized profiles. These profiles depend on the surface heat and momentum fluxes and the mixing depth, which can either be measured or estimated from routine observations such as, for example, wind speed near the surface, insolation, cloudiness, and temperature. At most sites, the fluxes and the mixing depth probably would have to be estimated due to the lack of direct measurements. Here, we summarize the methods used to estimate the fluxes, the mixing depth, and the profiles; most of these methods have been obtained from previous investigations.

1) SURFACE HEAT AND MOMENTUM FLUXES

The surface sensible heat flux, H, can be determined from the energy balance at the earth's surface (Oke 1978):

$$R_n = H + LE + G_s \tag{5}$$

where R_n is the net radiation, LE is the latent heat flux, and G_s is the soil heat flux. This general relationship is used for both daytime in which R_n is dominated by the insolation and nighttime when R_n is determined largely by the outgoing longwave radiation. Storage and advection of energy are neglected in this equation. Consequently, it is expected to be least accurate during sunrise or sunset transition periods when surface temperatures are changing most rapidly, or during postfrontal situations when significant cold or warm air advection is occurring.

In daytime, the net radiation R_n is found from a surface radiation budget formula suggested by Holtslag and van Ulden (1983):

$$R_n = \frac{(1 - r)R + c_1T^6 - \sigma T^4 + c_2N}{1 + c_3} \tag{6}$$

where R is the solar insolation, r is the surface albedo (expressed as a fraction), T is the air temperature, N is the cloud cover (expressed as a fraction), and σ is the Stefan–Boltzmann constant, 5.67×10^{-8} W m^{-2} K^{-4}. Holtslag and van Ulden assumed $c_1 = 5.31 \times 10^{-13}$ W m^{-2} K^{-6} and $c_2 = 60$ W m^{-2} based on other studies and derived $c_3 = 0.12$ from observations in The Netherlands. In the absence of measurements, the solar insolation is calculated from the Holtslag and van Ulden (1983) expression

$$R = ((990 \text{ W m}^{-2}) \sin\nu - 30 \text{ W m}^{-2})(1 - b_1 N^{b_2}) \quad (7)$$

where ν is solar elevation angle and the dimensional constants are appropriate for temperate sites at mid-latitude. The parameters b_1 and b_2 are empirical coefficients derived from observations of solar insolation during conditions with varying cloudiness; we assume $b_1 = 0.75$ and $b_2 = 3.4$.

The albedo is relatively constant for solar elevation angles, ν, above 30°, but increases for lower angles (Coulson et al. 1971; Iqbal 1983). We derived an empirical expression for the albedo, r, versus the solar elevation angle, ν, that gives a reasonable fit to the data of Iqbal (see Hanna et al. 1986) and have used it in determining R_n. It is

$$r = r' + (1 - r')e^{a\nu + b_2} \quad (8)$$

where r' is the albedo for $\nu = 90°$, $a = -0.1$, and $b_2 = -0.5(1 - r')$.

Using the observed insolation, we find that the predicted R_n from Eqs. (6) and (8) is in good agreement with observations at the Kincaid plant; e.g., the correlation coefficient between the predicted and observed R_n values is 0.985, and the root-mean-square (rms) deviation between the two is 42.9 W m^{-2} (see Hanna et al. 1986).

Given the net radiation, R_n, the sensible heat flux, H, is obtained from the expression of Holtslag and van Ulden (1983):

$$H = \left(\frac{(1 - \alpha) + (\gamma/s)}{1 + (\gamma/s)}\right)(R_n - G_s) - \alpha\beta' \quad (9)$$

where α is an empirical surface moisture parameter ranging from 0 to 1, $\beta' = 20$ W m^{-2}, $G_s = 0.1R_n$, $s = dq_s/dT$, q_s is the saturation specific humidity, $\gamma = c_p/\lambda$, c_p is the specific heat of air, and λ is the latent heat of water vaporization. The ratio γ/s varies with temperature, T, in the manner listed below

T(°C)	−5	0	5	10	15	20	25	30	35
γ/s	2.01	1.44	1.06	0.79	0.60	0.45	0.35	0.27	0.21

Holtslag and van Ulden found that α was 1 for a grass-covered surface in The Netherlands and was 0.45 for a moderately dry surface in the U.S. (in the Prairie Grass experiment).

The assumption that the ground heat flux G_s is 10% of the net radiation flux R_n is valid only for grassy fields. For desert areas, G_s may be as much as 30% of R_n, and for forests, G_s may be as low as 1% of R_n. In urban areas, G_s is sometimes equal to R_n.

Given the definitions of latent and sensible heat fluxes in the Holtslag and van Ulden method, the following expression for the surface moisture parameter, α, can be derived:

$$\alpha = \frac{(1 + \gamma/s)(0.9R_n)}{(1 + Br)[0.9R_n + \beta'(1 + \gamma/s)]} \quad (10)$$

where Br is the Bowen ratio

$$Br = \frac{H}{LE} \quad (11)$$

During daytime, Br is usually positive with values ranging from 0.1 for water bodies, to 1 for temperate grasslands, and as large as 10 for deserts. In HPDM, the Bowen Ratio is estimated by month for certain wind direction sectors, as a function of surface type and general climatological data (see Hanna et al. 1986). For each hour, an estimate of the moisture parameter, α, is made from Eq. (10), which is then substituted into Eq. (9) to calculate the sensible heat flux, H.

Using the sensible heat flux, H, the Holtslag and van Ulden (1983) method calculates a neutral friction velocity, u_{*_n}, and a Monin–Obukhov length, L, using the following equations:

$$u_{*_n} = 0.4u/\ln(z/z_0) \quad (12)$$

$$L = -u_*^3 T\rho c_p/(0.4gH) \quad (13)$$

The friction velocity, u_*, equals the square root of the surface momentum flux divided by ρ. For daytime conditions, the following Eq. (14), and Eq. (13) are iterated over u_* and L until the desired accuracy of L is reached, using ψ_m as the stability correction. These formulas are suggested by Businger et al. (1971):

$$u_* = 0.4u/(\ln(z/z_0) - \psi_m) \quad (14)$$

where

$$\psi_m = 2\ln(0.5(1 + \Phi_m^{-1})) + \ln(0.5(1 + \Phi_m^{-2})) - 2\arctan(\Phi_m^{-1}) + \pi/2 \quad (15)$$

and

$$\Phi_m = (1 - 15z/L)^{-1/4} \quad (16)$$

Because Eq. (12) neglects the displacement length, it should not be applied to sites where the wind speed is observed near the tops of trees or other large roughness elements. Also, it should be pointed out that Eq. (13) neglects the contribution of water vapor to buoyancy. This omission has less than a 10% effect on the calculated L (Briggs 1985).

At night, when the atmosphere is stable, the Weil–Brower (1984) method is used to calculate the heat and momentum fluxes and the Monin–Obukhov length. It is assumed that $\psi_m = -\beta z/L = -4.7z/L$ in Eq. (14). A scaling temperature, θ_*, is defined by the relation:

$$\theta_* = -H/(\rho c_p u_*) \quad (17)$$

Our methods of estimating θ_* are guided by observations reported by van Ulden and Holtslag (1985) which show that $\theta_* \propto u_*^2$ at small u_*, $\theta_* \sim$ constant at moderate u_*, and $\theta_* \propto u_*^{-1}$ at very large u_*. A first estimate of the scaling temperature θ_* is made using Holtslag and van Ulden's (1982) empirical equation for the moderate u_* region:

$$\theta_{*_1} = (0.09 \text{ K})(1 - 0.5N^2) \quad (18)$$

where N is the fractional cloud cover and θ_* has units of Kelvins. Note that this equation implies that the scaling temperature is a constant at night under clear skies. A second estimate of θ_* for the small u_* region is made by setting $2u_0/C_{DN}^{1/2}u = 1$ in Eq. (20) below. This results in:

$$\theta_{*_2} = TC_{DN}u^2/(4\beta_m zg) \quad (19)$$

where the neutral drag coefficient C_{DN} is defined as $0.4/\ln(z/z_0)$ and β_m is a constant 4.7. This limit will produce the minimum possible L from Eq. (20) and thus, combined with the θ_* from Eq. (18), will define a maximum range on θ_*. Then θ_* is set equal to the smaller of θ_{*_1} and θ_{*_2}.

From Eq. (17) it is seen that the sensible heat flux, H, is proportional to the product of u_* and θ_*. For large values of u (or u_*), where θ_{*_1} is smaller than θ_{*_2}, an additional check on the product $u_*\theta_*$ must be made, since the heat flux H does not keep increasing indefinitely with higher wind speeds. Here H is limited by the isothermal net radiation, Q', which is arbitrarily taken as -50 watts/m^2. Thus, equating $H = -\rho c_p u_* \theta_*$ with Q', the value of θ_* is not allowed to exceed $0.05/u_*$, where all parameters are expressed in MKS units.

During stable conditions, when $\psi_m = -\beta_m z/L$ in Eq. (14), a quadratic equation in u_* results and an analytical solution for u_* is possible:

$$u_* = \frac{C_{DN}u}{2}\left[1 + \left(1 - \left(\frac{2u_0}{C_{DN}^{1/2}u}\right)^2\right)^{1/2}\right] \quad (20)$$

where

$$u_0 = (\beta_m zg\theta_*/T)^{1/2} \text{ and } C_{DN} = 0.4/\ln(z/z_0) \quad (21)$$

For real solutions, the following condition must be met:

$$2u_0/(C_{DN}^{1/2}u) \leq 1 \quad (22)$$

If this condition does not hold, L is set to a default minimum of 5 m in HPDM and u_* is calculated with that assumption. Otherwise, L is calculated from Eq. (13).

From these procedures, estimates of H, u_*, L, and θ_* for all stabilities are made within HPDM. The minimum set of input data consists of wind speed at a single height, time of day (to calculate the sun's elevation angle), and cloudiness. If other observations are available (such as ground heat flux or net radiation), they can be subsututed for the default assumptions used above.

2) MIXING DEPTH, h

Observations of mixing depth, h, should be used if available and if there is expected to be little error. Our experiences at the Kincaid site (see Table 2) suggest that observations of h tend to have an error of ±20% during the afternoon and ±100% during the nighttime and transition periods. These mixing depth observations were made by Doppler Acoustic Sounder (DAS) and by slowly rising minisondes, and the errors were determined by intercomparisons of mixing depths estimated by three different meteorologists from the different observing methods. These observations have much uncertainty in the mid-to-late morning period when maximum ground-level concentrations are observed.

If observed mixing depths are unavailable or unreliable, analytical formulas for the mixing depth are used in HPDM. For stable conditions, the Nieuwstadt (1981) interpolation formula was first tested:

$$(h/L) = \frac{-1 + (1 + 2.28u_*/fL)^{1/2}}{3.8} \quad (23)$$

which approaches the limit $h = 0.3u_*/f$ in neutral conditions ($L \to \infty$). The Coriolis parameter, f, which equals 10^{-4} sec^{-1} at midlatitudes is included in this equation mainly because a time scale is needed in a dimensional argument, rather than because it has any physical significance. For unstable conditions, the Carson (1973) prognostic equation for h is used, as modified by Weil and Brower (1984). This procedure depends on estimation of the surface heat flux, H, and the magnitude of the temperature gradient in the capping inversion, and produces a rising mixing depth during the morning as heat is added to the boundary layer. The Carson unstable mixing depth estimate does not necessarily approach the limit $h = 0.3u_*/f$ in neutral conditions ($L \to -\infty$). Furthermore, neither this formula nor any other theoretical formula can adequately treat the breakdown of the inversion during the late afternoon.

Initial testing of Eq. (23) in HPDM showed poor model performance in high-wind nearly-neutral conditions. An independent dataset consisting of over 200 h of SO_2 concentration observations during high-wind conditions ($u > 8$ m s^{-1}) at five power plants was available for model testing (see section 4*b* for a more complete description of these data). The observed maximum SO_2 GLCs showed no significant variability

from stable to unstable conditions. However, Eq. (23) predicts a rapid drop in the mixing depth between neutral conditions and slightly stable conditions (e.g., for $u_* = 0.5$ m s^{-1}, the predicted neutral $h = 0.3u_*/f \approx 1500$ m; but for $u_* = 0.5$ m s^{-1} and $L = 100$ m the predicted $h \approx 225$ m). Because the stack height is about 200 m and plume rise is on the order of 100 m, the plume centerline height for $u_* = 0.5$ m s^{-1} and $L = 100$ m is above the mixing height predicted by Eq. (23), and GLCs predicted by the dispersion model are therefore very low.

To produce agreement between observations and model predictions of GLCs during high-wind conditions, the predicted mixing depth should be sufficiently above the predicted plume elevation that it does not affect the plume dispersion. For these reasons, the default assumption is made in HPDM that $h = 0.3u_*/f$ for high-wind neutral conditions. For the purposes of calculating ground-level concentrations, neutral conditions are defined in HPDM by $L > 100$ m on the stable side and by a method proposed by Golder (1972) on the unstable side. The Golder method uses boundary layer theory to assign limits to L for certain roughness lengths and Pasquill stability classes. Perhaps in the future, researchers can work towards the development of a method for predicting mixing depth that provides a smooth transition from unstable to stable conditions and is consistent with observations of vertical dispersion of tall stack plumes in high-wind conditions. HPDM currently has a discontinuity in h as L passes through approximately -100 or 100 m. For example, when $L = 101$ m, h is assumed to equal $0.3u_*/f$, and when $L = 99$ m, h is given by Eq. (23).

In practice, any definitions of mixing depth that involve the friction velocity, u_*, and hence the Monin–Obukhov length, L, will experience difficulties during light-wind cloudy conditions. Wind observations become highly uncertain at values near the threshold of the instrument, and therefore any calculations of u_*, L, and h are equally uncertain. The threshold or starting speeds of anemometers used for routine observations are typically on the order of 1 m s^{-1}. Consequently it is expected that the boundary layer parameterization in this section will be most accurate during moderate to high-wind neutral conditions rather than during light-wind neutral conditions. This problem during light-wind neutral conditions has limited impact on comparisons with observed maximum GLCs, since the plume will rise high into the atmosphere and disperse to the ground relatively slowly at those times.

3) Wind speed profile

If observations of wind speed at plume elevation are not available, the Businger et al. (1971) wind speed profile formulas (14–16) are used to extrapolate to stack top elevation during unstable conditions. For stable conditions, the wind speed profile formula reduces to a simple log–linear relation:

$$u = \frac{u_*}{0.4}\left[\ln\left(\frac{z}{z_0}\right) + 4.7\left(\frac{z}{L}\right)\right] \quad (z/L > 0) \quad (24)$$

Theoreticians suggest that this formula may break down at about $z = L$, above which the profile tends to a purely linear form. We assume that it is valid up to the top of the nocturnal boundary layer ($h \sim 5L$). Because comprehensive observations and models are not available for the wind speed in the upper part of the PBL for all stability conditions, the wind speed is assumed to be constant at heights above the nocturnal boundary layer [from Eq. (23)] or the highest measurement level (whichever is higher). The model can also accommodate observed wind data if they extend above stack top elevation.

4) Potential temperature profile

In some rare cases, temperature profiles may be observed at heights where the plume is located and would be input directly to the model. The following procedures are used if these data are not available:

If conditions are unstable, HPDM sets $d\theta/dz$ to zero at plume elevation. Otherwise, the Stull (1983) scaling formula is used:

$$(d\theta/dz)_2/(d\theta/dz)_1 = \exp[-0.77(z_2/H_T - z_1/H_T)] \quad (25)$$

where it is assumed in HPDM that the scale height H_T equals the pbl height h, as observed or as predicted by Eq. (23). Note that an observation or prediction of $d\theta/dz$ at some level (z_1) is needed in order to estimate $d\theta/dz$ at another level (z_2).

If no $d\theta/dz$ is observed at any level, the model creates one in the surface layer using an equation suggested by Businger et al. (1971):

$$d\theta/dz = (\theta_*/0.4z)(0.74 + 4.7z/L). \quad (26)$$

A height of $z_1 = 50$ m would be used in this procedure, and the resulting $(d\theta/dz)_1$ would be input to Eq. (25). This part of the model has not been adequately tested, since the Kincaid and Bull Run plumes never produced significant ground level concentrations during stable conditions.

5) Turbulence formulas

If the turbulence components σ_v and σ_w are observed at stack elevation the model uses these observations directly. Otherwise, it calculates the turbulence components internally by means of analytical formulas. With the exception of dual doppler acoustic sounders or extremely tall towers, current technology is inadequate for making routine observations of turbulence at heights of 200 to 300 m. Our experience with the Doppler Acoustic Sounders at the Kincaid and Bull Run experimental sites suggests that these turbulence measurements are unreliable. Consequently, the theo-

retical formulas for turbulence are likely to be used in all instances at tall stacks. Hicks' (1985) interpolation formulas for hourly averaged turbulence components are used in HPDM for nearly neutral conditions with positive sensible heat flux:

$$\sigma_{w_0} = (1.20u_*^2 + 0.35w_*^2)^{1/2} \quad (27)$$

$$\sigma_{v_0} = (3.60u_*^2 + 0.35w_*^2)^{1/2} \quad (28)$$

where subscript "0" refers to conditions near the ground surface. Predictions of these formulas were shown by Hicks to agree quite well with observations at a number of field sites. The p.d.f. and convective scaling models assume that σ_w and σ_v are constant with height within the mixed layer ($0 \leq z \leq h$). If the plume is completely above the mixing height in unstable conditions, the turbulence parameters σ_w and σ_v are arbitrarily set equal to 0.1 times their surface values. There is no information in the literature on the values of σ_w and σ_v above the mixed layer and the transition layer, but as this information becomes available, HPDM should be modified, where appropriate.

Initially, HPDM was tested using the following theoretical formulas for the turbulence parameters in slightly stable and stable conditions (Hanna, Briggs, and Hosker 1982):

Slightly stable ($L \geq 100$ m):

$$\sigma_w/u_* = 1.3 \exp(-2fz/u_*) \quad (29)$$

$$\sigma_v/u_* = 2.0 \exp(-2fz/u_*) \quad (30)$$

Stable ($L < 100$ m):

$$\sigma_v/u_* = 1.3(1 - z/h) \quad (31)$$

$$\sigma_v/u_* = 2.0(1 - z/h) \quad (32)$$

This set of theoretical formulas did not produce good agreement with SO_2 GLCs observed during the high-wind experiments (see Section 4*b*). Consequently, sets of effective turbulence parameters were defined that produce the best estimates of GLCs from tall stacks during the high-wind conditions that were investigated in this project.

Slightly stable ($L \geq 100$ m):

$$\sigma_w = 0.5\sigma_{w_0} \quad (33)$$

$$\sigma_v = 0.7\sigma_{v_0} \quad (34)$$

Stable ($L < 100$ m):

$$\sigma_w = 1.3u_{*_0} \quad (35)$$

$$\sigma_v = \max(1.5u_{*_0}, 0.5 \text{ m s}^{-1}) \quad (36)$$

These formulas are recommended for stack heights above 100 m. The 0.5 m s^{-1} minimum in Eq. (36) accounts for meandering that occurs over an hourly period and has been found to be valid at several experiments in a variety of locations (Hanna et al. 1985). The $L = 100$ m criterion for the dividing point between slightly stable and stable conditions is the same as that specified in section 3.2. These formulas apply only to tall stack plumes within the mixed layer. For plumes above the mixed layer, the arbitrary assumptions $\sigma_w = 0.1\sigma_{w_0}$ and $\sigma_v = 0.1\sigma_{v_0}$ are made, as before. Equations (33) through (36) represent effective turbulence parameters as they relate to dispersion of plumes from tall stacks towards the ground, and it is not implied that these turbulence parameters would be observed by an anemometer at stack height. Furthermore, since the GLC is also a strong function of plume rise, these optimum estimates of σ_w and σ_v are tied to the plume rise equation (see Eq. 58) that applies in these conditions.

b. Vertical dispersion in unstable conditions

Here HPDM has two options for the vertical term, G_z, in the dispersion equation (Eq. 2) for unstable conditions: a probability density function (p.d.f.) model developed from the Weil and Brower (1985) paper, and a convective scaling model described by Hanna and Paine (1987). These formulas for unstable conditions are more important than the formulas for stable or neutral conditions at Kincaid and Bull Run because maximum observed ground-level concentrations were observed during unstable conditions at those sites. The p.d.f. model is so named because it accounts for the known non-Gaussian p.d.f. of vertical velocities in the convective boundary layer (Briggs 1985, Weil 1985). It is used to predict the crosswind-integrated concentration, C_y, which is equal to the $(Q/u)G_z$ product in Eq. (2). The p.d.f. model is used in HPDM for low buoyancy fluxes, defined by $F_* < 0.1$, where the dimensionless buoyancy flux is defined by

$$F_* = F/uw_*^2h \quad (37)$$

where

$$F = w_r R_r^2 (g/T_p)(T_p - T_a) \quad (38)$$

and w_r is initial plume vertical speed, R_r is initial plume radius, g is the acceleration of gravity, T_p is initial plume temperature and T_a is ambient temperature. The parameter F is commonly referred to as the plume buoyancy flux.

The scaling parameter, F_*, is approximately proportional to the ratio of the plume rise in convective conditions to the mixing depth. For $F_* < 0.1$, the upper part of the plume does not touch the top of the mixed layer and the ground-level concentration can be predicted by integrating over an assumed analytical formula for the vertical velocity p.d.f. This p.d.f. is the sum of two Gaussian distributions—one for the updrafts and one for the downdrafts. It is assumed that downdrafts occur 60% of the time. The dispersion parameter, σ_z, is assumed to be a function of the buoyant

plume rise and the turbulent dispersion. The following solution is obtained:

$$C_y uh/Q = (0.48/\sigma_{z_1}^*)\exp(-h_1^{*2}/2\sigma_{z_1}^{*2}) + (0.32/\sigma_{z_2}^*)\exp(-h_2^{*2}/2\sigma_{z_2}^{*2}) \quad (39)$$

where

$$\sigma_{zi}^{*2} = 0.21F_*^{2/3}X_*^{4/3} + b_i^2X_*^2 \quad (40)$$

$$h_i^* = h_s^* + 1.6F_*^{1/3}X_*^{2/3} + a_iX_* \quad (41)$$

$i = 1$ or 2, $h_s^* = h_s/h$, $\sigma_{zi}^* = \sigma_{zi}/h$, and $X_* = w_*x/uh$

The parameter h_s is the stack height. The constants $a_1 = -0.35$, $a_2 = 0.4$, $b_1 = 0.24$ and $b_2 = 0.48$ are related to the vertical velocity p.d.f. Subscripts 1 and 2 refer to the downdrafts and updrafts, respectively. The F_* term in Eq. (40) contains the contribution to σ_z due to buoyancy effects. Material that reaches the upper boundary, h, is assumed to disperse downward according to a Gaussian formula. In order to obtain point concentrations from the predictions of cross-wind integrated concentration, C_y, Eq. (39) must be multiplied by the horizontal term, G_y, Eq. (3), with σ_y in the p.d.f. model given by:

$$\sigma_y/h = 0.56X_*/(1 + 0.7X_*)^{1/2} \text{ (p.d.f. model)} \quad (42)$$

As the dimensionless buoyancy parameter, F_*, approaches 1 or greater, the plume interacts more and more with the stable air capping the mixed layer. A convective scaling formula (Hanna and Paine 1987) is used in HPDM for extreme light-wind convective conditions with $F_* > 1$:

$$C_{max} = 0.4(Q/F)w_*^2(h - h_s)/h^2 \quad (43)$$

where C_{max} is the maximum GLC anywhere on the network. This type of scaling formula was suggested by Briggs (1985), although we have substituted the term $(h - h_s)/h^2$ for $1/h$ in his formula. This substitution is necessary for tall stacks, where the buoyant plume begins rising from a height that is a significant fraction of the mixing depth. The model implicitly accounts for plume lofting into low capping inversions and subsequent reentrainment of plume material into the mixed layer. Note that Eq. (43) is independent of wind speed and hence gives a solution even if the wind speed approaches zero. To calculate concentrations at any specific position, the following simple convective scaling formulas are used for C_y and σ_y:

$$C_y uh/Q = 0.056X_*/F_* \quad \text{for} \quad X_*/F_* \leq 10 \quad (44)$$

$$C_y uh/Q = \exp(-(7F_*/X_*)^{3/2}) \quad \text{for} \quad X_*/F_* > 10 \quad (45)$$

$$\sigma_y/h = 0.6X_*. \quad \text{(convective scaling model)} \quad (46)$$

Equation (43) was tested with the Bull Run data by Hanna and Paine (1987) with the results shown in Fig. 4. The maxima observed and predicted C/Q agree within ±10%, but the correlation among all the points is not significantly different from zero.

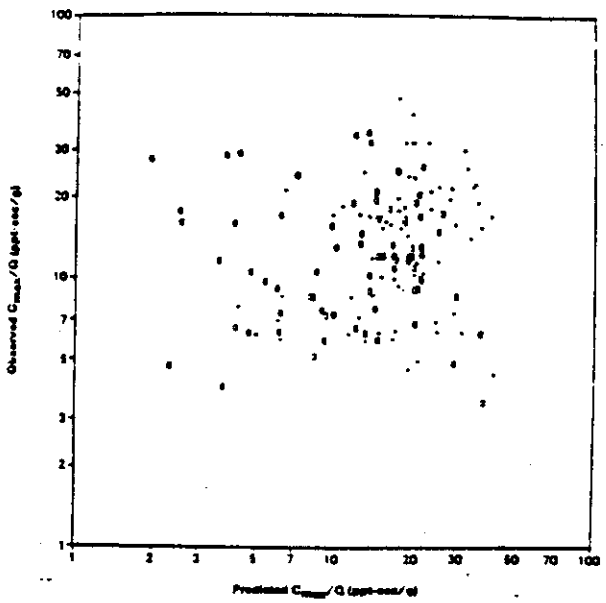

FIG. 4. Observed and predicted normalized hourly maximum ground-level concentration C_{max}/Q, for Kincaid (circles) and Bull Run (crosses) evaluation data.

c. *Dispersion in neutral and stable conditions*

The Gaussian formula is used for horizontal dispersion for all stabilities and for vertical dispersion for neutral and stable conditions. The total dispersion, σ, is assumed to be the quadratic sum of the component due to plume buoyancy, $\sigma_b = \Delta h/3.5$, and the turbulent component, σ_y or σ_z. The parameter Δh is the plume rise above the stack top elevation. The turbulent components are given by the formulas (Hanna et al. 1977):

$$\sigma_v = \sigma_v x f_y(x/uT_{L_y})/u \quad (47)$$

$$\sigma_z = \sigma_w x f_z(x/uT_{L_z})/u \quad (48)$$

where σ_v and σ_w are turbulent components, f_y and f_z are dimensionless functions, and T_{L_y} and T_{L_z} are Lagrangian time scales for dispersion. If σ_v and σ_w are not observed, they are predicted by Eqs. (33) through (36).

The functions f_y and f_z are given by:

$$f_y = \{1 + 0.9[x/(u \times 15\,000 \text{ s})]^{1/2}\}^{-1} \quad (49)$$

$$f_z = [1 + x/(2uT_{L_z})]^{-1/2} \quad (50)$$

The form of f_y is based on a study by Hanna (1986), who found that a time scale T_{L_y} of 15 000 sec provided a best fit to observations of lateral dispersion of plumes from sources with stack heights of about 200 m. Draxler (1976) first suggested this f_y equation, but assumed that the time scale was 1000 sec based on observations

of plumes from sources at heights closer to the ground surface. The vertical Lagrangian time scale T_{L_z} is given by the formulas:

Stable:

$$T_{L_z} = z/\sigma_w \quad (\text{if } z \leq L) \tag{51}$$

$$T_{L_z} = 0.27s^{-1/2} \quad (\text{if } L < 10 \text{ m}) \tag{52}$$

$$T_{L_z} = (z/\sigma_w)(L - 10 \text{ m})/(z - 10 \text{ m}) + 0.27s^{-1/2}(z - L)/(z - 10 \text{ m}) \quad (\text{if } 10 \text{ m} < L < z) \tag{53}$$

Slightly Unstable:

$$T_{L_z} = 0.27(z/\sigma_w)(0.55 - 0.38z/|-L|) \quad (\text{if } z \leq |-L|) \tag{54}$$

$$T_{L_z} = (0.3h/\sigma_w)[1 - \exp(-5z/h)] - 0.0003 \exp(8z/h) \quad (\text{if } |-L| < z < h) \tag{55}$$

where s equals $(g/T)\cdot(d\theta/dz)$. Equations (51), (54), and (55) were suggested by Hanna, Briggs, and Hosker (1982) and are based on boundary layer observations. Equations (54) and (55) are used in HPDM for slightly unstable conditions (unstable class "D" as defined by Golder 1972). The T_{L_z} asymptote for stable conditions (Eq. 52) is a slight modification of Hunt's (1982) suggestions. Equation (53) is an interpolation between Eqs. (51) and (52) and should be further tested with independent data.

d. Plume rise and partial penetration of elevated inversions

The p.d.f. and convective scaling model options contain implicit procedures for treating plume rise. For neutral and stable conditions, plume rise and inversion penetration are calculated explicitly by HPDM using formulas in this section. Plume rise, Δh, is assumed to be given by the minimum of the predictions of the following set of standard equations:

Bent-over stable

$$\Delta h = 2.6(F/us)^{1/3} \tag{56}$$

Calm stable

$$\Delta h = 4F^{1/4}s^{-3/8} \tag{57}$$

Final transitional

$$\Delta h = 38.7F^{3/5}u^{-1} \tag{58}$$

Unstable break-up

$$\Delta h = 4.3(F/u)^{3/5}H^{-2/5} \tag{59}$$

Neutral break-up

$$\Delta h = 1.3(F/uu_*^2)(1 + h_s/\Delta h)^{2/3} \tag{60}$$

where H is the surface heat flux in units of $m^2\ s^{-3}$, calculated using formulas in Section 3*a*. Briggs (1984) discusses most of these plume rise options, and the "final transitional" option is the equivalent of a formula in the MPTER model, assuming high initial plume buoyancy flux.

If the plume rise, Δh, calculated from these procedures exceeds 0.67 times the distance $(h - h_s)$ to the mixing depth, then the top of the plume impacts the capping inversion, partial plume penetration of the inversion is expected, and a new estimate of plume rise, Δh_t, is made using Eq. (57) and a default potential temperature gradient $d\theta/dz = 0.5°C/100$ m. This default value is half of what Weil and Brower (1984) used in their PPSP model, and is necessary to prevent overpredictions of GLCs discovered for the PPSP model (Tikvart et al. 1987). The 0.67 factor is derived from the assumption that plume radius is proportional to 0.5 times plume rise; consequently the top edge of the plume first bumps the inversion when $\Delta h = (h - h_s)/1.5$. The fraction, P, of plume mass that penetrates the inversion is given by

$$P = 1 \quad \text{if} \quad (h - h_s)/\Delta h_t \leq 0.5 \tag{61}$$

$$P = 1.5 - (h - h_s)/\Delta h_t \quad \text{if} \quad 0.5 < (h - h_s)/\Delta h_t < 1.5 \tag{62}$$

The effective plume rise of the portion $(1 - P)$ of the plume trapped below h is calculated from the formula:

$$\Delta h = (0.62 + 0.38P)(h - h_s), \tag{63}$$

which is based on lidar observations reported by Weil and Bower (1984). Given new values of source strength, $Q(1 - P)$, and plume elevation, $h_s + \Delta h$, the standard Eq. (2) is used to calculate the downwind distribution of ground-level concentrations.

Many researchers are currently working on the partial penetration or lofting problem, and it is expected that improved formulas for this phenomenon will soon become available. Because of the modular format of HPDM, modifications to the code can easily be made.

4. Evaluation of HPDM

HPDM has been evaluated using field data from the Kincaid and Bull Run power plants and from a selected high-wind dataset from five power plants. These two evaluation exercises are described below.

a. Kincaid and Bull Run datasets

Details concerning the field experiments at the Kincaid and Bull Run sites were discussed in section 2, and maps of the monitor locations are given in Figs. 1 through 3.

1) PROCEDURES FOR MODEL EVALUATION

About 200 h of SF_6 data are available in the independent datasets from each site and about 120 days of

SO_2 data are available from Kincaid in the evaluation database. The days in the evaluation database were not used at all in the development phase of this project. Recognizing the large errors in model predictions due to wind direction uncertainties (Smith 1984), it was decided to restrict the model evaluation to the maximum observed and predicted concentrations during each hour on each monitoring arc. In any given experiment, there were typically about five monitoring arcs operating. Thus the observed and predicted values are paired in space to the extent that they are the same distance from the source, but they may be at different angular positions. In the results given below the following statistics are calculated (Hanna and Heinold 1985):

$$\text{Mean Bias} = \bar{C}_p - \bar{C}_o \quad (64)$$

Normalized Mean Square Error (NMSE)

$$= \overline{(C_p - C_o)^2}/\bar{C}_p\bar{C}_o \quad (65)$$

$$\text{Correlation } r = \overline{(C_p - \bar{C}_p)(C_o - \bar{C}_o)}/\sigma_{C_p}\sigma_{C_o} \quad (66)$$

$$\text{Percent of } C_p \text{ within a factor of two of } C_o \quad (67)$$

where an overbar indicates an average, and subscripts p and o represent predicted and observed values, respectively. In addition the following attributes of the unpaired concentration distributions are studied: maximum overall concentration, and the average of top 25 concentrations ($\bar{C}$ (Top 25)).

Confidence limits on these statistics (except for the maximum) for individual models and the differences between the statistics for pairs of models are calculated by estimating a p.d.f. of the statistic using the bootstrap resampling procedure (Efron 1982). The bootstrap procedure is very useful because it is nonparametric; i.e., it does not rely on a specified distribution function for the concentrations. If the p.d.f.s were parametric (e.g., Gaussian), standard statistical tests such as the student t or chi-square could be used to determine confidence intervals. The bootstrap is best explained using a simple example. Suppose a set of 100 pairs of observed and predicted concentrations are available, and $\bar{C}_o$ and $\bar{C}_p$ are calculated. Suppose the statistic of interest is the mean bias, $\bar{C}_p - \bar{C}_o$. In the bootstrap procedure, 100 new pairs are selected randomly (with replacement) by computer from the original set and new values of $\bar{C}_o$ and $\bar{C}_p$ are calculated. This is done 100 to 1000 times (depending on the computer costs and availability), giving a histogram or p.d.f. of the statistic $\bar{C}_p - \bar{C}_o$. If all of the resampled values of $\bar{C}_p - \bar{C}_o$ are, say, greater than zero, then it can be stated with great confidence that $\bar{C}_p - \bar{C}_o$ is significantly different from zero. But if the resampled $\bar{C}_p - \bar{C}_o$ distribution crosses zero at some point between the 2.5th and 97.5th percentiles, then it cannot be stated with 95% confidence that $\bar{C}_p - \bar{C}_o$ is significantly different from zero.

The bootstrap can be applied to any of the statistics listed in Eqs. (64) through (67). However, any statistical procedure is limited by its underlying assumption that the data are independent, which is not strictly true for these data. Because the data are somewhat correlated from one hour to the next, the effective number of degrees of freedom will be less than the number of data points, the true variance of the population will be underestimated, and hence the statistical significance of model differences will be underestimated. In addition the estimation of confidence intervals is limited by the maximum value in the observed distributions; this is more important for statistics near the tails than near the center of a distribution.

2) Results for Kincaid and Bull Run

The model evaluation procedures described above were applied to the evaluation database at Kincaid and Bull Run. The MPTER model and the HPDM model were tested. Turbulence values (σ_v and σ_w) observed at the 100 m level of meteorological towers at each site were used in HPDM where required. Mixing depths predicted by the Carson–Weil–Brower method were used for the SF_6 data hours and observed National Weather Service (NWS) mixing depths (based on airport data) were used for the SO_2 data hours. Calculations of 1-h SF_6 concentrations and 1-h, 3-h, and 24-h averaged SO_2 concentrations were made. Note that the concentrations were normalized by the source strength, Q, in all these calculations.

The results for the maximum concentration (unpaired) and the average over the top 25 concentrations are given in Table 3. The calculation of 95% confidence limits on the $\overline{C/Q}$ (top 25) values yields the following results:

- HPDM predicted values of $\overline{C/Q}$ (top 25) are not significantly different from the observed values for the SF_6 Kincaid 1 h and the SO_2 Kincaid 24-h datasets.
- HPDM and MPTER model predictions of $\overline{C/Q}$ (top 25) are not significantly different from each other for the SF_6 Kincaid 1-h and the SO_2 Kincaid 1-h datasets.

It can be concluded that the two models have similar performance when tested with the SF_6 Kincaid data, although HPDM is closer to the overall maximum. The maximum is underpredicted by 3% by HPDM and overpredicted by MPTER by 8%.

At Bull Run, where light-wind convective conditions prevailed, the MPTER predictions of $\overline{C/Q}$ (top 25) are low by about a factor of 2, while the HPDM predictions are within 15% of the observations. The maximum $\overline{C/Q}$ at Bull Run is overpredicted by 13% by HPDM and underpredicted by 33% by MPTER. The MPTER model underpredictions at Bull Run are probably due to the model's neglect of partial penetration of the capping inversion. On many hours, the MPTER model calculates that $\Delta h/(h - h_s) > 1$ and therefore assumes that the plume never comes to the ground.

TABLE 3. Results of Evaluation of Top 25 Model Predictions. [C/Q, in units of $(s/m^3) \times 10^{-6}$]

Dataset	C/Q Max			$\overline{C/Q}$ (top 25)		
	Obs	MPTER	HPDM	Obs	MPTER	HPDM
SF_6 Kincaid 1h	208	225	202	130	133	131
SF_6 Bull Run 1 h	338	225	383	197	87	170
SO_2 Kincaid 1 h	269	280	264	160	143	145
SO_2 Kincaid 3 h	161	117	129	83	65	87
SO_2 Kincaid 24 h	76	56	55	38	23	38

The evaluation of the top 25 SO_2 data subset at Kincaid suggest that HPDM and MPTER perform equally well (accuracy of about ±10%) for 1 h averages, but that MPTER underpredicts by more and more as the averaging time increases. An examination of the $\overline{C/Q}$ (top 25) results for the 24 h averages shows that MPTER underpredicts by 40% while HPDM matches the observed value exactly. The progressively worse underprediction by MPTER as averaging time increases is due to the increasing influence of neutral conditions, for which MPTER is known to underpredict (see section 4*b*).

The results of the application of the model performance measures to the maximum C/Q on monitoring arcs for each hour in the evaluation dataset are given in Table 4. The observations and predictions are paired in time and in radial distance from the stack. The number of elements (n) in each dataset is listed. Values of the four performance measures given in Eqs. (64)–(67) are listed for both models, along with results of the application of the bootstrap procedure for estimating confidence limits (listed in rows A and B). We note that even though the concentration data at any site tend to be log-normally distributed, the bootstrap confidence limits do not depend on the concentration p.d.f. It is seen that both models underpredict the mean C_o/Q at both sites for both tracers, with MPTER about 15% to 80% low and HPDM about 5% to 40% low. The best performance for the models occurs for the Kincaid SF_6 data, where the predictions by the two models of the mean C/Q are not significantly different at the 95% confidence level. Part of the discrepancy for SO_2 at Kincaid may be due to the fact that the background is ignored.

The biggest difference between the models shows up in the NMSE statistic, where the MPTER model has the poorer performance for every dataset. HPDM has an NMSE of about 0.9 for the Kincaid SF_6 data and the Kincaid SO_2 24-h average data (i.e., the root-mean-square error is about equal to the mean).

The correlation coefficients are seen to be not very useful for comparing model performance, since they are quite low (at most, $r^2 = 22\%$ of the variance is explained), and there is no significant difference (at the 95% level) between the correlation coefficients for

TABLE 4. Results of evaluation of models for maximum concentration on monitoring arcs [C/Q in units of $(s/m^3) \times 10^{-6}$]. Subscript M indicates MPTER and Subscript H indicates HPDM.

Performance measure	SF_6 1 h		Kincaid SO_2		
	Kincaid n = 175	Bull Run n = 158	1 h n = 2880	3 h n = 960	24 h n = 120
$\overline{C_o/Q}$	59.5	80.4	20.4	18.0	13.6
$\overline{C_M/Q} - \overline{C_o/Q}$	−8.3	−65.4	−11.4	−10.4	−7.7
$\overline{C_M/Q} - \overline{C_o/Q}$	−3.6	−31.3	−6.9	−6.1	−4.5
A* (zero bias test)	H				
B** (zero bias difference test)	M–H		n.a.†	n.a.	
$NMSE_M$	1.22	7.10	4.85	3.18	1.72
$NMSE_H$	.90	1.78	2.82	1.95	.83
B** (zero NMSE difference test)			n.a.	n.a.	
r_M	.06	.25	.33	.39	.38
r_H	.06	.31	.41	.47	.43
A* (zero r test)	M, H				
B** (zero r difference test)	M–H	M–H	n.a.	n.a.	M–H
% FAC 2 (M)	45	13	10	17	28
% FAC 2 (H)	49	33	18	22	45
B** (zero FAC 2 difference test)	M–H		n.a.	n.a.	

* Row A: Models for which the statistic is not significantly different from 0 at the 95% confidence level.

** Row B: Cases where the difference in the statistic is not significantly different from 0 at the 95% confidence level.

† n.a.: Bootstrap procedure not applied to this case, since the number of cases is very large.

the models for any given dataset. MPTER tends to have the lower correlation, but it is not significantly lower.

The "percent within a factor of 2" statistic indicates that HPDM is significantly better than MPTER for Bull Run SF_6 and Kincaid SO_2 24-h averages. The magnitude of this statistic is not as high as one would hope, with a median value of 33% for HPDM and 17% for MPTER.

The scatter of individual ratios of predicted to observed concentrations is large for both models, with standard deviations on the same order as the mean. Figures 5 and 6 contain values of individual C_p/C_o for the maximum hourly concentrations at Bull Run, plotted as a function of mixing depth, h, for the HPDM and MPTER models, respectively. The large number of $C_p/C_o = 0$ cases in Fig. 6 for the MPTER model at low mixing depths reflects the failure of the model to account for plume material remaining in the mixed layer during periods when the plume rises up to or above the mixing depth. The data in Fig. 5 illustrate that HPDM has eliminated much of this problem. There is little bias of C_p/C_o with mixing depth for HPDM, and about 40% of the points are within the range from 0.5 to 2.0 (i.e., factor of 2 accuracy).

Tables 3 and 4 and Figs. 5 and 6 suggest that HPDM may be a significant improvement over the MPTER model, which is the recommended EPA model for tall stacks in flat or rolling terrain. The biggest improvements occur for 1-h average concentrations during light-wind convective conditions (Bull Run SF_6 data) and for long-term averages when nearly neutral conditions are important (Kincaid SO_2 24-h data). In most

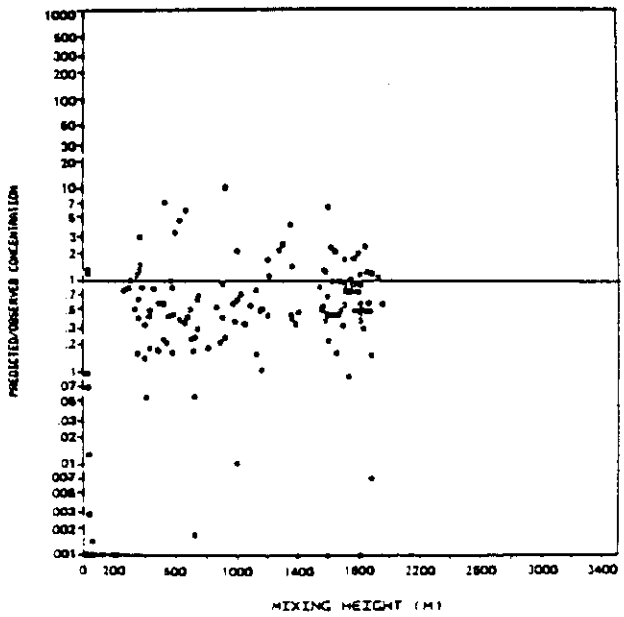

FIG. 5. Residual plot showing C_p/C_o versus mixing depth for HPDM predictions at Bull Run.

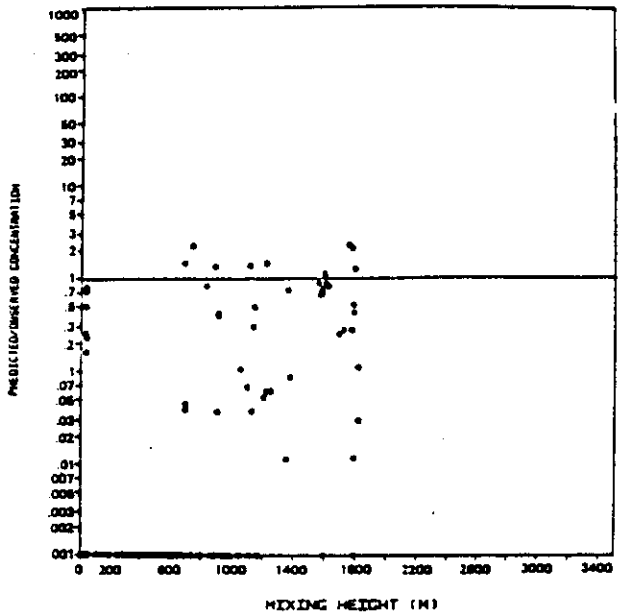

FIG. 6. Residual plot showing C_p/C_o versus mixing depth for MPTER predictions at Bull Run.

cases, there is a significant difference (at the 95% confidence level) between the MPTER model and HPDM. The absolute highest SF_6 concentrations are predicted by HPDM with an accuracy of 15% or less.

b. Evaluation of HPDM with high wind dataset

The Kincaid and Bull Run datasets include very few high-wind periods. High GLCs can occur around power plant stacks during periods with high winds due to the reduced plume rise and enhanced rate of vertical dispersion associated with these conditions (Hanna, Briggs and Hosker 1982). This problem is more severe when the stack height is 100 m or less. In order to thoroughly test the modules in HPDM for high-wind, nearly neutral conditions, an independent dataset from SO_2 monitoring networks around five separate power plants was used. This section describes the dataset and the results of the model evaluation exercise. In all cases, turbulence observations were not available and turbulence intensities were calculated using the default formulas in HPDM.

A set of 264 h of high-wind data was available as a result of a previous study (Paine and Venkatram 1983; Venkatram and Paine 1985). A summary of the characteristics of this dataset is given in Table 5. Hours were included in the dataset from the five power plant sites if the observed speed exceeded 8 m s^{-1}. In a few cases, this criterion was relaxed somewhat if the wind shear at plume level was strong. At Baldwin and Clifty Creek, an additional criterion imposed was that the maximum observed SO_2 GLC must exceed about 250 $\mu g/m^3$. Thus, in each of the 264 h, there was a good

TABLE 5. Summary of characteristics of high-wind dataset.

Plant Name	Baldwin (Illinois)	Clifty Creek (Indiana)	Dickerson (Maryland)	Chalk Point (Maryland)	Morgantown (Maryland)
Megawatts	1800	1300	555	710	1150
Stacks	184 m (three)	208 m (three)	122 m (two)	122 m (two)	213 m (two)
Period studied	4/1978–3/1980 4/1982–4/1983	1974–1977	1972–1975	1972–1975	1972–1975
SO_2 Monitors*	Up to 5 fixed monitors	One fixed monitor	Mobile van	Mobile van	Mobile van
Roughness	0.2 m	0.2 m	0.3 m	0.3 m	0.3 m
Terrain	Flat	In valley	Rolling	Flat	Flat
Hours of data	157	79	13	9	6

* Data from monitors is included only if high concentrations are observed. Sometimes as many as five monitors show high concentrations at Baldwin; only one shows high concentrations at Clifty Creek; and only one point is extracted from the mobile van data at the three Maryland power plants.

chance that the concentration near the plume centerline was sampled. Because the observations at the three Maryland Power Plants were taken as part of a special field program, there are only 28 h available, but the data are generally of high quality (Weil 1977). The maximum observed hourly averaged concentration in the total set is 1048 $\mu g/m^3$ and the mean over all hours and all monitors is 325 $\mu g/m^3$.

HPDM and the MPTER model were both run for these datasets, with the results shown in Table 6. Statistics are calculated for the following data subsets:

- All hours, all monitors (600 monitor hours)
- All hours, maximum monitor (264 monitor hours)
- Stable hours, all monitors (200 monitor hours)
- Stable hours, maximum monitor (97 monitor hours)
- Unstable hours, all monitors (380 monitor hours)
- Unstable hours, maximum monitor (167 monitor hours)

The data are separated into stable and unstable hours because the models sometimes use different algorithms to estimate turbulence and diffusion in these cases.

The statistics that are employed for the evaluation in Table 6 are the mean bias and the normalized mean-square error, NMSE. The maximum and mean of the top ten concentrations are also evaluated because of their regulatory significance.

Table 6 shows that HPDM performs quite well for all datasets, whereas MPTER underpredicts by a factor of about five, on average. In nearly all cases, the HPDM performance measure is significantly better than the MPTER performance measure. The exception is that MPTER does as well as HPDM in predicting the top ten concentrations in unstable conditions. There is not a significant difference (at the 95% confidence level) between the two models in this case. These few hours when MPTER does well happen to be those classified by the model as stability class C (3). As soon as class D (4) is used in MPTER, it consistently underpredicts. It may be that MPTER would be better if class C dispersion curves were used wherever class D stability is indicated with strong winds, although this change was not tested. In any event, HPDM does equally well for both stable and unstable high-wind hours. Its normalized mean-square error (NMSE) is about unity for all data and about 0.4 for the maximum monitor dataset.

TABLE 6. Evaluation of HPDM and MPTER for high wind dataset. (Concentrations are in $\mu g/m^3$.)

Datasets	C_o (max)	C_p (max)		$(\overline{C_p - C_o})$ (top 10)		$(\overline{C_p - C_o})$ (all data)	
		HPDM	MPTER	HPDM	MPTER	HPDM	MPTER
All Hours	1048	1198	1109	6*	17*	−75	−258
Stable Hours	1045	863	193	−120	−741	−116	−316
Unstable Hours	1048	1198	1109	60*	83*	−49	−224

NMSE (all data)		$(\overline{C_p - C_o})$ (Max monitor)		NMSE (Max monitor)		Number of cases: All monitors	Number of cases: (Max monitors)
HPDM	MPTER	HPDM	MPTER	HPDM	MPTER		
1.10	6.2	−90	−379	.40	4.4	600	264
1.25	15.8	−128	−489	.34	8.8	220	97
1.04	4.4	−67	−314	.45	3.2	380	167

* If an asterisk appears next to a pair of numbers, then the difference between models is not significantly different from zero at the 95% confidence level.

In other words, the rms error for HPDM is less than or equal to the mean. In contrast, the NMSE for MPTER is in the range from about 5 to 15 for these cases, mostly due to its large underpredictions. The MPTER model's prediction of the overall maximum concentration during stable concentrations is only 18% of the observed value, indicating that the model underestimates vertical dispersion in those conditions.

Table 6 shows that there is little difference in observed GLCs between stable and unstable conditions. This result led to the conclusion that the high-wind (neutral) dispersion algorithm in HPDM should be independent of whether conditions were slightly unstable or slightly stable. Consequently, HPDM will predict similar ground level concentrations for both positive and negative values of L such that $|L| > 100$ m.

c. *Sensitivity of HPDM to externally specified parameters*

The maximum ground level concentrations predicted by HPDM are dependent on four externally specified meteorological parameters: the mixing depth h, the capping inversion strength $d\theta/dz$, the friction velocity u_* and the sensible heat flux H. There is at least a 10% to 20% error in the specification of any of these parameters, and sometimes (e.g., periods with advection or rapid local variability with time) this error grows to a factor of 2 or more. We have studied the sensitivity of the model to variations in the sensible heat flux caused by variations in ground moisture conditions, finding that maximum concentrations increase by about 20% to 30% if the ground moisture is decreased from "typical temperate" to "dry". With dry conditions, turbulence is increased and the plume is brought to the ground faster. Similarly, if the capping inversion strength is increased from 0.005°C/m to 0.01°C/m, the maximum concentrations increase by a factor of about two, due to less penetration of the inversion by the plume. When the mixing depth is close to the plume elevation, errors of a factor of 2 in mixing depth can greatly modify the calculated plume concentration factor, and thus can cause an order of magnitude difference in ground level concentration predictions.

Although we have not conducted a comprehensive study of HPDM sensitivity to these meteorological parameters, our limited analysis verifies the finding that the uncertainty in HPDM predictions is quite high for specific places and times. A more detailed study could better pinpoint the expected uncertainty. However, when looking at the sets of observations and predictions unpaired in space and time (e.g., maximum concentration observed and predicted anywhere on the Kincaid monitoring network over the entire duration of the experiment), the agreement is fairly good. Apparently, we are satisfactorily modeling the joint distribution of the parameters h, $d\theta/dz$, u_*, and H, even though we cannot accurately model their individual values for a given place and time. This conclusion is consistent with that reached by other investigators (Smith 1984; Weil 1985).

5. Conclusions

The Hybrid Plume Dispersion Model (HPDM) has been developed following suggestions by Hanna et al. (1977), Smith (1984), Weil (1985), and others who recommend that applied dispersion models should be updated to reflect current knowledge of atmospheric boundary layers and dispersion. For example, state-of-the-art procedures for estimating surface fluxes of heat and momentum based on simple wind and radiation measurements and site characteristics have been incorporated. Convective scaling principles have been used as the basis for a simplified model of vertical dispersion in the daytime. Lofting of buoyant plumes into elevated capping inversions is accounted for. Since sophisticated instrumentation is usually not available to provide detailed meteorological input, the model has various default options that will use limited observations (e.g., wind speed at a single level, cloudiness, and time of day) to internally generate the required parameters. In some cases, such as the specification of vertical profiles of turbulence, the parameters that were assumed represent those that provide the optimum agreement with observed GLCs.

The model is developed specifically for buoyant plumes from tall stacks in relatively flat terrain (hill height less than about one-half stack height). It is also assumed that building-induced downwash is a minor effect. Because the highest GLCs from these sources in flat terrain occur during light-wind convective conditions (i.e., summer afternoons) with relatively low mixing depths, HPDM model development has emphasized these conditions. The model is expected to perform best for short-term averages (1 to 3 h) during strong convection, and is expected to be least successful during stable nighttime conditions. However, buoyant plumes from stacks with heights of 100 m or greater in flat terrain do not show significant GLCs during stable conditions. This conclusion is quite different for stacks located in terrain where the hill heights are greater than the stack height.

The greatest improvement of HPDM over the reference EPA model (MPTER or CRSTER) is seen for high-wind neutral conditions, where the EPA model underpredicts by a factor of two or more, while HPDM is shown to be accurate within ±20%. For the same reason, HPDM is more accurate for long-term averages (24 h or greater), since nearly-neutral hours make up most of the average. During convective conditions at Kincaid where winds were usually moderate (5 to 10 m s^{-1}), the MPTER model and HPDM can both simulate the observed maximum concentration quite well (+20%). However, during very convective conditions

at Bull Run, where winds were very light (2 m s^{-1} or less), MPTER underpredicts the maximum concentrations by a factor of 2 since it permits too much of the plume to be lost in the capping inversion. An examination of data from all hours shows that HPDM generally shows a smaller mean bias and NMSE, although the difference between these performance measures for the models is sometimes not significant (at the 95% confidence level).

The surface heat and momentum flux calculations made within HPDM are based on the assumption of a ground surface that is grass, agricultural, or forested. The ground moisture is assumed to be at the low end of the typical range for the Kincaid and Bull Run sites, since both field experiments took place during drought conditions. It was found that the maximum predicted concentration could vary by ±30% depending on the ground moisture assumption (more ground moisture leads to lower sensible heat fluxes and hence lower vertical dispersion). However the highest observed concentrations were found to be well-correlated with dry conditions, and these periods contributed heavily to the top 25 data subset. More research is needed on this sensitive parameter.

To conclude, HPDM is recommended for use for the following conditions:

- Buoyant plumes from stacks at least 100 m tall.
- Terrain heights less than one-half stack height.
- Cases where building-induced downwash is not important.
- Sites where convection is strong or winds are high and the ground surface is grass, agricultural, or forested.

In the future, research will be performed to generalize the model for other conditions. The first effort will involve including the effects of an urban surface. In addition, a crude terrain correction factor (like that in MPTER) will be installed for future testing.

Acknowledgments. This research was supported by the Electric Power Research Insitute, with Dr. Glenn Hilst as project manager. Some of the analysis was done by Cynthia Burkhart and Michael Dennis of ERT, Inc., and Roger Brower and Lou Corio of VERSAR, Inc. We appreciate the contributions of Dr. Jeffrey Weil of CIRES in developing the p.d.f. approach and in reviewing drafts of this manuscript.

REFERENCES

Berkowicz, R., Olesen, H. R., and U. Torp, 1985: The Danish Gaussian air pollution model (OML). Description, test and sensitivity analysis in view of regulatory applications. *Proc. NATO 15th Int. Tech. Meeting on Air Poll. Modelling and Its Application.*

Bowne, N. E., R. J. Londergan and D. R. Murray, 1985: Summary of results and conclusions for the EPRI plume model validation project: moderately complex site. EA-3755, EPRI, Palo Alto, CA 94304.

——, ——, —— and H. S. Borenstein, 1983: Overview, results and conclusions for the EPRI plume model validation project: plains site. EA-3074, EPRI, Palo Alto, CA 94304.

Briggs, G. A., 1975: Plume Rise Predictions, in *Lectures on Air Pollution and Environmental Impact Analyses*, Amer. Meteor. Soc., Boston, MA, 59–111.

——, 1984: Plume rise and buoyancy effects. *Atmosphere Science and Power Production*, D. Randerson, Ed., DOE/TIC-27601, 327–366.

——, 1985: Analytical parameterizations of diffusion: the convective boundary layer. *J. Climate Appl. Meteor.*, 24, 1167–1186.

Businger, J. A., J. C. Wyngaard, Y. Izumi and E. F. Bradley, 1971: Flux-profile relationships in the atmospheric surface layer. *J. Atmos. Sci.*, 28, 181–189.

Carson, D. J., 1973: The development of a dry inversion-capped convectively unstable boundary layer. *Quart. J. Roy. Meteor. Soc.*, 99, 450–467.

Coulson, K. L., and D. W. Reynolds, 1971: The spectral reflectance of natural surfaces. *J. Appl. Meteor.*, 10, 1285–1295.

Draxler, R. R., 1976: Determination of atmospheric diffusion parameters. *Atmos. Environ.*, 10, 99–105.

Efron, B., 1982: *The jackknife, the bootstrap and other resampling plans.* Soc. Ind. and Appl Math., CBMMS-NSF-38 92 pp.

Golder, D., 1972: Relations among stability parameters in the surface layer. *Bound.-Layer Meteor.*, 13, 47–58.

Gryning, S. E., A. A. M. Holtslag, J. S. Irwin and B. Sivertsen, 1987: Applied dispersion modelling based on meteorological scaling parameters. *Atmos. Environ.*, 21, 79–90.

Hanna, S. R., 1986: Lateral dispersion from tall stacks. *J. Climate. Appl. Meteor.*, 25(10), 1426–1433.

——, and D. W. Heinold, 1985: Development and application of a simple method for evaluating air quality models. API Pub. No. 4409, Am. Pet. Inst., Washington, DC, 38 pp.

——, and R. J. Paine, 1987: Convective scaling applied to diffusion of buoyant plumes. *Atmos. Environ.*, 21, 2153–2162.

——, G. A. Briggs and R. P. Hosker, 1982: *Handbook on atmospheric diffusion.* U.S. Department of Energy DOE/TIC-11223, 102 pp.

——, J. C. Weil and R. J. Paine, 1986: Plume model development and evaluation, hybrid approach. Final Report No. D034-500, EPRI, Palo Alto, CA.

——, L. L. Schulman, R. J. Paine, J. E. Pleim and M. Baer, 1985: Development and evaluation of the offshore and coastal diffusion model. *J. Air Poll. Control Assoc.*, 35, 1039–1047.

——, G. A. Briggs, J. Deardorff, B. A. Egan, F. A. Gifford and F. Pasquill, 1977: AMS workshop on stability classification schemes and sigma curves—Summary of recommendations. *Bull. Amer. Meteor. Soc.*, 58, 1305–1309.

Hayes, S. R., and G. E. Moore, 1986: Air quality model performance: a comparative analysis of 15 model evaluation studies. *Atmos. Environ.*, 20, 1897–1911.

Hicks, B. B., 1985: Behavior of turbulence statistics in the convective boundary layer. *J. Climate Appl. Meteor.*, 24, 607–614.

Holtslag, A. A. M., and A. P. Van Ulden, 1982: Simple estimates of nighttime surface plumes from routine weather data. Scientific Report 82-4, Royal Netherlands Meteorological Institute, deBilt.

——, and A. P. Van Ulden, 1983: A simple scheme for daytime estimates of the surface fluxes from routine weather data. *J. Climate Appl. Meteor.*, 22, 517–529.

Hunt, J. C. R., 1982: Diffusion in the stable boundary layer. *Atmos. Turb. and Air Poll. Modeling*, F. T. M. Nieuwstadt and H. van Dop, Eds., D. Reidel, 231–274.

——, 1985: Diffusion in the stably stratified atmospheric boundary layer. *J. Clim. Appl. Meteor.*, 24, 1187–1195.

Iqbal, Muhammad, 1983: *An Introduction to Solar Radiation.* Academic Press, p. 286.

Liu, M. K., and G. E. Moore, 1984: Diagnostic validation of plume models at a plains site. EA-3077, EPRI, Palo Alto, CA.

Moore, G. E., M. K. Liu and R. G. Londergan, 1985: Diagnostic validation of Gaussian and first-order closure plume models at a moderately complex terrain site. EA-3760, EPRI, Palo Alto, CA.

Nieuwstadt, F. T. M., 1981: The steady-state height and resistance

laws of the nocturnal boundary layer: Theory compared with Cabauw observations. *Bound.-Layer. Meteor.*, 20, 3–17.
Oke, T. R., 1978: *Boundary Layer Climates.* Wiley & Sons, 372 pp.
Paine, R., and A. Venkatram, 1983: Modeling tall stack releases in high wind conditions. Task 1: assembly of model evaluation data base. Environmental Research and Technology, Inc. for Maryland Power Plant Siting Program, Dept. of Natural Resources, Rep. No. P-B846-100.
Petersen, G., D. Eppel and H. Grassl, 1987: Verification of the pollutant transport model 'MODIS' using EPRI plains site data from a tall stack. *Bound.-Layer Meteor.*, 41, 265–278.
Pierce, T. E., 1986: An evaluation of a convective scaling parameterization for estimating the diffusion of a buoyant plume. *Proc. NATO 16th Int. Tech. Meeting on Air Poll. Modelling and Its Applic.*
Smith, M. E., 1984: Review of the attributes and performance of 10 rural diffusion models. *Bull. Amer. Meteor. Soc.*, 65(6), 554–558.
Stull, R. B., 1983: Integral scales for the nocturnal boundary layer. Part 1: Empirical depth relationships. *J. Climate Appl. Meteor.*, 22, 673–686.
Tikvart, J. A., J. L. Dicke and J. S. Touma, 1987: Including new modeling techniques in regulatory programs. At APCA Annual Meeting, Paper 87-73.1 16 pp.
Turner, D. B., T. Chico and J. Catalano, 1986: TUPOS—A multiple source Gaussian dispersion algorithm using on-site turbulence data. EPA/600/8-86/010, USEPA, Research Triangle Park, North Carolina, 38 pp.
Van Ulden, A. P., and A. A. M. Holtslag, 1985: Estimation of atmospheric boundary layer parameters for diffusion applications. *J. Clim. Appl. Meteor.*, 24, 1196–1207.
Venkatram, A., 1980: Dispersion from an elevated source in the convective boundary later. *Atmos. Environ.*, 14, 1–10.
——, and R. J. Paine, 1985: A model to estimate dispersion of elevated releases into a shear-dominated boundary layer. *Atmos. Environ.*, 19, 659–667.
Weil, J. C., 1977: Evaluation of the gaussian plume model at Maryland power plants. Martin Marietta Laboratories for Maryland Power Plant Siting Program, Dept. of Natural Resources, Rep. No. PPSP-MP-16.
——, 1985: Updating applied diffusion models. *J. Clim. Appl. Meteor.*, 24, 1111–1130.
——, and R. P. Brower, 1984: An updated gaussian plume model for Tall Stacks. *J. Air Pollut. Control Assoc.*, 34, 818–827.
Weil, J. C., and L. A. Corio, 1985: Dispersion formulations based on convective scaling. Maryland Power Plant Siting Program, Maryland Department of Natural Resources, Annapolis, MD. Report No. PPRP-MP-60.
——, L. A. Corio and R. P. Brower, 1986: Dispersion of buoyant plumes in the convective boundary layer. *Proc. Fifth Joint Conf. on Appl. of Air Poll. Meterol.*, Boston, MA, Amer. Meteor. Soc., 335–338.